

# Four octamolybdate compounds with properties of organic dye adsorption and photocatalytic reduction of Cr(VI)

Xinxin Hao, Jun Ying\*, Yanping Zhang, Aixiang Tian, Mengle Yang, Xiuli Wang\*

## Experimental

### Materials and General Methods

All reagents and solvents used in the synthetic process are purchased from commercial channels and need no further purification before use. The FT-IR spectra were recorded on a Magna FT-IR 560 spectrometer (KBr tablet) with a test range of 4000–400  $\text{cm}^{-1}$ . The solid-state diffuse-reflectance UV–vis spectra were recorded on a PerkinElmer Lambda 750 UV–vis spectrometer equipped with an integrating sphere. The powder X-ray diffraction (PXRD) diagram was obtained on a Ultima IV with D/teX Ultra diffractometer, and the UV–Vis absorption spectrum was obtained by using the UV–1801 ultraviolet spectrophotometer. The electrochemical measurements were performed with a CHI660 electrochemical workstation. In addition, the traditional three-electrode system was used in this experiment, in which platinum wire and saturated calomel electrode (SCE) were used as counter electrode and reference electrode respectively. The title compounds modified carbon paste electrodes (CPEs) and glassy carbon electrodes (GCE) were used as the working electrodes.

### Preparation of compounds 1–4

#### Synthesis of $[\text{Co}(\text{HPtpm})_2(\beta\text{-Mo}_8\text{O}_{26})_{0.5}(\xi\text{-Mo}_8\text{O}_{26})_{0.5}]\cdot\text{H}_2\text{O}$ (1)

A mixture of  $\text{MoO}_3$  (0.1 g, 0.69 mmol),  $\text{CoSO}_4\cdot 7\text{H}_2\text{O}$  (0.1 g, 0.36 mmol), ptpm (0.02 g, 0.07 mmol) and  $\text{H}_2\text{O}$  (10 mL) was stirred for 2 h in air at room temperature. The pH of the mixture was adjusted to about 1.85 by the addition of 0.1 M  $\text{HNO}_3$  solution. Then, the suspension was transferred to a Teflon-lined autoclave and kept at 140 °C for 6 days. The temperature was reduced to room temperature with a rate of 10 °C per hour. After washing with distilled water, a large number of orange block crystals **1** can be obtained (yield 28% based on Mo). Anal. calcd. for  $\text{C}_{28}\text{H}_{42}\text{CoMo}_8\text{N}_{10}\text{O}_{29}$  (1809.14): C 18.59, H 2.34, N 7.74%. Found: C 18.55, H 2.28, N 7.81%.

#### Synthesis of $[\text{Co}(\text{HPtpm})_2(\delta\text{-Mo}_8\text{O}_{26})]\cdot\text{H}_2\text{O}$ (2)

The synthetic method of **2** was the same as that of **1**. When **1** was generated, a small amount of orange–yellow massive crystal **2** was generated (yield 8% based on Mo). Anal. calcd. for  $\text{C}_{28}\text{H}_{42}\text{CoMo}_8\text{N}_{10}\text{O}_{29}$  (1809.14): C, 18.59; H, 2.34; N, 7.74%. Found: C, 18.52; H, 2.29; N, 7.83%.

In order to obtain a large number of compound **2**, we tried other synthetic methods. A mixture of  $\text{Na}_2\text{MoO}_4\cdot 2\text{H}_2\text{O}$  (0.1 g, 0.41 mmol),  $\text{CoSO}_4\cdot 7\text{H}_2\text{O}$  (0.1 g, 0.36 mmol), ptpm (0.02 g, 0.07 mmol) and  $\text{H}_2\text{O}$  (10 mL) was stirred for 2 h in air at room temperature. The pH of the mixture was adjusted to about 3.70 by the addition of 0.1 M  $\text{HNO}_3$  solution. Then, the suspension was transferred to a Teflon-lined autoclave and kept at 160 °C for 5 days. The temperature was reduced to room temperature with a rate of 10 °C per hour. After washing with distilled water, a large number of orange–yellow massive crystal **2** can be obtained (yield 27% based on Mo).

### Synthesis of [Co(HPtpm)<sub>2</sub>(β-Mo<sub>8</sub>O<sub>26</sub>)] (3)

The synthetic method of **3** was the same as that of **1**, except that the pH value of the solution was adjusted to 2.35. After slow cooling to room temperature, yellow block crystals of compound **3** were isolated and washed with distilled water (yield 30% based on Mo). Anal. calcd. for C<sub>28</sub>H<sub>40</sub>CoMo<sub>8</sub>N<sub>10</sub>O<sub>28</sub> (1791.11): C, 18.78; H, 2.25; N, 7.82%. Found: C, 18.72; H, 2.16; N, 7.90%.

### Synthesis of [Zn(HPtpm)<sub>2</sub>(β-Mo<sub>8</sub>O<sub>26</sub>)] (4)

**Method 1:** **4** was synthesized in the same way as **3**, except that ZnSO<sub>4</sub>·7H<sub>2</sub>O (0.1 g, 0.35 mmol) was used instead of CoSO<sub>4</sub>·7H<sub>2</sub>O. After slow cooling to room temperature, white block crystals of **4** were isolated and washed with distilled water (yield 29% based on Mo). Anal. calcd. for C<sub>28</sub>H<sub>40</sub>Mo<sub>8</sub>N<sub>10</sub>O<sub>28</sub>Zn (1797.60): C 18.71, H 2.24, N 7.79. Found: C 18.64, H 2.30, N 7.86.

**Method 2:** A mixture of (NH<sub>4</sub>)<sub>6</sub>Mo<sub>7</sub>·4H<sub>2</sub>O (0.1 g, 0.08 mmol), ZnSO<sub>4</sub>·7H<sub>2</sub>O (0.1 g, 0.35 mmol), ptpm (0.02 g, 0.07 mmol) and H<sub>2</sub>O (10 mL) was stirred for 2 h in air at room temperature. The pH of the mixture was adjusted to about 3.72 by the addition of 0.1 M HNO<sub>3</sub> solution. Then, the suspension was transferred to a Teflon-lined autoclave and kept at 150 °C for 7 days. The temperature was reduced to room temperature with a rate of 10 °C per hour. White block crystals of **4** were obtained with distilled water (yield 30% based on Mo).

### Preparation of bulk-modified CPEs of compounds 1 to 4

The carbon paste electrode (1-CPE) modified by compound **1** was prepared as follows: a mixture of compound **1** (0.01 g) and graphite powder (0.10 g) was ground for about 20 minutes using agate mill. While stirring, 0.1 mL of liquid paraffin was added to the obtained mixture. Then the mixture was stuffed into a glass tube with an inner diameter of 1.5 mm, and the surface of the glass tube was wiped with weighing paper.

### Preparation of glassy carbon electrode of compounds 1 to 4

The glassy carbon electrode (1-GCE) modified by compound **1** was prepared as follows: 5 mg compound **1** and 5 mg acetylene black in the mass ratio of 1:1 were mixed and ground in a mortar for 40 minutes. Weigh 4 mg of the mixture, add 0.5 mg of deionized water and 10 μL of naphthalene solvent, and ultrasonicate for 1 hour to form slurry. Dropping the suspension onto the surface of glass carbon electrode, and drying at room temperature for 2 hours. Then 5 μL of naphthalene solution was added dropwise to continue drying. In the same way, **2**-, **3**- and **4**-GCEs were prepared using compounds **2**-**4**.

### Dye adsorption and desorption test

In this work, cationic dyes Crystal Violet (CV), Methylene Blue (MB), Neutral Red (NR), Rhodamine B (RhB) and anionic dye Methyl Orange (MO) were selected. The adsorption effect of compounds **1**-**4** on the above dyes was studied. 20 mg samples of compounds **1**-**4** were dispersed in 30 mL aqueous solution containing different dyes. The obtained mixed solution was put in a light-proof container and stirred. 3 mL Sample of the solution at regular intervals, then use a UV-1801 ultraviolet spectrophotometer to detect the sample. In addition, we also studied the selective adsorption of dyes. The operation method was similar, except that a binary dye mixture was used. The desorption experiment was to soak the adsorbed compounds in acetonitrile solution for ultrasonic treatment so as to be reused in the next operation.

## X-ray Crystallographic Study

X-ray diffraction analysis data for compounds **1–4** were collected at 293 K by using Bruker Smart Apex CCD diffractometer with MoK $\alpha$  ( $\lambda = 0.71073 \text{ \AA}$ ). All crystal structures were solved by direct method, and refined on  $F^2$  by full matrix least square method using OLEX software package.<sup>1</sup> Table 1 lists the crystal data and structural refinement of compounds **1–4**. Table S1 lists the selected key lengths ( $\text{\AA}$ ) and angles ( $^\circ$ ) of **1–4**. CCDC numbers: 2213004 (**1**), 2261537 (**2**), 2261538 (**3**), 2261540 (**4**).

## FT-IR spectra and PXRD

Fig. S6 shows the IR spectra of compounds **1–4**. In the spectra of **1–4**, the characteristic peaks at 426–935 $\text{cm}^{-1}$ , 433–935 $\text{cm}^{-1}$ , 419–929 $\text{cm}^{-1}$  and 419–943 $\text{cm}^{-1}$  are attributed to  $\nu(\text{Mo-O}_t)$  and  $\nu(\text{Mo-O}_{b/c}\text{-Mo})$ . The characteristic peaks in the region of 1096–1648  $\text{cm}^{-1}$  for **1**, 1082–1646  $\text{cm}^{-1}$  for **2**, 1090–1655  $\text{cm}^{-1}$  for **3**, 1090–1641  $\text{cm}^{-1}$  for **4** are attributed to ptpm ligands.

The experimental diffraction peaks of powder X-ray diffraction (PXRD) of **1–4** are consistent with the simulated diffraction peaks. This shows that the phase purity of the sample is good, as shown in Figure. S7.

## Solid-state diffuse-reflection study

We measured the optical diffuse reflectance spectra of solid samples **1–4** at room temperature in order to determine the energy gap of these four materials, and we then calculated the absorption data using the kubelka–munk function. The linear portion of the absorption edge was extrapolated to produce the band gap ( $E_g$ ) estimates: 1.89 eV for **1**, 1.81 eV for **2**, 1.89 eV for **3** and 3.23 eV for **4**. The above results confirmed the semiconductor properties of the title compounds (Figure. S8).

**Table S1.** Crystal data and structure refinement for compounds **1–4**.

	<b>1</b>	<b>2</b>	<b>3</b>	<b>4</b>
Empirical formula	C <sub>28</sub> H <sub>42</sub> CoMo <sub>8</sub> N <sub>10</sub> O <sub>29</sub>	C <sub>28</sub> H <sub>42</sub> CoMo <sub>8</sub> N <sub>10</sub> O <sub>29</sub>	C <sub>28</sub> H <sub>40</sub> CoMo <sub>8</sub> N <sub>10</sub> O <sub>28</sub>	C <sub>28</sub> H <sub>40</sub> Mo <sub>8</sub> N <sub>10</sub> O <sub>28</sub> Zn
Formula weight	1809.14	1809.14	1791.11	1797.60
Temperature/K	296.15	296.15	296.15	296.15
Crystal system	triclinic	triclinic	triclinic	triclinic
Space group	P-1	P-1	P-1	P-1
<i>a</i> / $\text{\AA}$	10.3922(8)	10.5624(4)	9.4250(3)	9.3723(3)
<i>b</i> / $\text{\AA}$	13.9362(12)	11.4680(4)	11.8401(4)	11.8323(3)
<i>c</i> / $\text{\AA}$	19.3170(17)	12.2785(5)	12.2595(4)	12.2768(4)
$\alpha$ / $^\circ$	110.942(2)	69.0330(10)	111.0120(10)	111.2900(10)
$\beta$ / $^\circ$	93.654(3)	67.3720(10)	107.6530(10)	107.6560(10)
$\gamma$ / $^\circ$	101.381(3)	74.1290(10)	93.4150(10)	93.1050(10)
Volume/ $\text{\AA}^3$	2533.8(4)	1265.89(8)	1194.98(7)	1187.90(6)
<i>Z</i>	2	1	1	1
$D_c$ (g·cm <sup>-3</sup> )	2.371	2.350	2.489	2.513
$\mu$ /mm <sup>-1</sup>	2.328	2.327	2.466	2.636
F(000)	1750.0	865.0	865.0	868.0

Goof on F <sup>2</sup>	1.195	1.046	1.010	1.111
R <sub>1</sub> <sup>a</sup> [I > 2σ(I)]	0.0337	0.0239	0.0340	0.0326
wR <sub>2</sub> <sup>b</sup> (all data)	0.0843	0.0627	0.0909	0.0842

<sup>a</sup>  $R_1 = \frac{\sum \|F_o\| - \|F_c\|}{\sum \|F_o\|}$ . <sup>b</sup>  $wR_2 = \left\{ \frac{\sum [w(F_o^2 - F_c^2)^2]}{\sum [w(F_o^2)^2]} \right\}^{1/2}$ .

**Table S2.** Selected bond distances (Å) and angles (°) for compounds **1–4**.

Compound 1			
Co(1)-O(4)	2.077(3)	Co(1)-N(6)	2.224(4)
Co(1)-N(3) <sup>3</sup>	2.095(4)	Co(1)-N(4)	2.075(3)
Co(1)-N(7)	2.036(4)	Co(1)-N(5)	2.176(4)
O(4)-Co(1)-N(3) <sup>3</sup>	92.79(13)	O(4)-Co(1)-N(6)	152.30(13)
O(4)-Co(1)-N(5)	85.47(13)	N(3) <sup>3</sup> -Co(1)-N(6)	91.89(15)
N(3) <sup>3</sup> -Co(1)-N(5)	173.67(15)	N(7)-Co(1)-O(4)	79.33(13)
N(7)-Co(1)-N(3) <sup>3</sup>	89.25(14)	N(7)-Co(1)-N(6)	73.45(14)
N(7)-Co(1)-N(4)	171.63(14)	N(7)-Co(1)-N(5)	96.40(14)
N(4)-Co(1)-O(4)	104.25(13)	N(4)-Co(1)-N(3) <sup>3</sup>	98.05(14)
N(4)-Co(1)-N(6)	102.09(14)	N(4)-Co(1)-N(5)	76.53(14)
N(5)-Co(1)-N(6)	92.46(15)	N(4)-N(3)-Co(1) <sup>3</sup>	124.2(3)
C(8)-N(3)-Co(1) <sup>3</sup>	128.8(3)	N(8)-N(7)-Co(1)	127.4(3)
Symmetry codes for 1: <sup>1</sup> -X,-Y,1-Z; <sup>2</sup> 1-X,-Y,-Z; <sup>3</sup> -X,1-Y,1-Z			
Compound 2			
Co(1)-O(2)	2.108(2)	Co(1)-O(2) <sup>2</sup>	2.108(2)
Co(1)-N(4) <sup>2</sup>	2.094(2)	Co(1)-N(4)	2.094(2)
Co(1)-N(5) <sup>2</sup>	2.094(2)	Co(1)-N(5)	2.094(2)
O(2)-Co(1)-O(2) <sup>2</sup>	180.0	N(4)-Co(1)-O(2)	91.33(9)
N(4) <sup>2</sup> -Co(1)-O(2)	88.67(9)	N(4)-Co(1)-O(2) <sup>2</sup>	88.67(9)
N(4) <sup>2</sup> -Co(1)-O(2) <sup>2</sup>	91.33(9)	N(4) <sup>2</sup> -Co(1)-N(4)	180.0
N(4) <sup>2</sup> -Co(1)-N(5)	102.64(10)	N(4) <sup>2</sup> -Co(1)-N(5) <sup>2</sup>	77.36(10)
N(4)-Co(1)-N(5) <sup>2</sup>	102.64(10)	N(4)-Co(1)-N(5)	77.36(10)
N(5)-Co(1)-O(2) <sup>2</sup>	89.16(9)	N(5) <sup>2</sup> -Co(1)-O(2) <sup>2</sup>	90.84(9)
N(5) <sup>2</sup> -Co(1)-O(2)	89.16(9)	N(5)-Co(1)-O(2)	90.84(9)
N(5) <sup>2</sup> -Co(1)-N(5)	180.0	N(3)-N(4)-Co(1)	137.2(2)
C(9)-N(4)-Co(1)	114.1(2)	C(10)-N(5)-Co(1)	117.1(2)
Symmetry codes: <sup>1</sup> 1-X,1-Y,2-Z; <sup>2</sup> 2-X,1-Y,1-Z			
Compound 3			
Co(1)-O(2) <sup>2</sup>	2.151(3)	Co(1)-O(2)	2.151(3)
Co(1)-N(4) <sup>2</sup>	2.047(4)	Co(1)-N(4)	2.047(4)
Co(1)-N(5)	2.147(4)	Co(1)-N(5) <sup>2</sup>	2.147(4)

O(2) <sup>2</sup> -Co(1)-O(2)	180.00(16)	N(4) <sup>2</sup> -Co(1)-O(2) <sup>2</sup>	85.05(13)
N(4) <sup>2</sup> -Co(1)-O(2)	94.95(13)	N(4)-Co(1)-O(2) <sup>2</sup>	94.95(13)
N(4)-Co(1)-O(2)	85.05(13)	N(4)-Co(1)-N(4) <sup>2</sup>	180.0(2)
N(4) <sup>2</sup> -Co(1)-N(5) <sup>2</sup>	77.06(14)	N(4)-Co(1)-N(5)	77.06(14)
N(4)-Co(1)-N(5) <sup>2</sup>	102.94(14)	N(4) <sup>2</sup> -Co(1)-N(5)	102.94(14)
N(5)-Co(1)-O(2)	94.82(13)	N(5) <sup>2</sup> -Co(1)-O(2)	85.18(13)
N(5)-Co(1)-O(2) <sup>2</sup>	85.18(13)	N(5) <sup>2</sup> -Co(1)-O(2) <sup>2</sup>	94.82(13)
N(5)-Co(1)-N(5) <sup>2</sup>	180.00(11)	N(3)-N(4)-Co(1)	134.0(3)
C(9)-N(4)-Co(1)	116.1(3)	C(10)-N(5)-Co(1)	115.6(3)

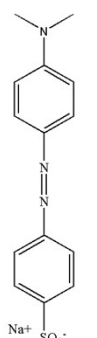
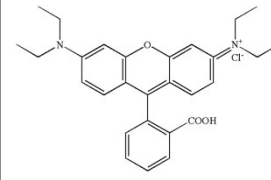
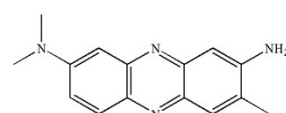
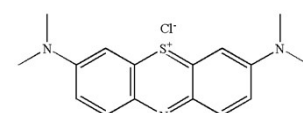
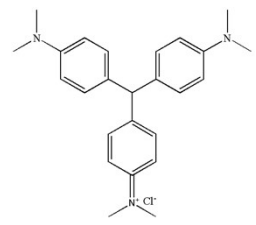
Symmetry codes: <sup>1</sup>1-X,2-Y,2-Z; <sup>2</sup>1-X,1-Y,2-Z

**Compound 4**

Zn(1)-O(2)	2.263(3)	Zn(1)-O(2) <sup>2</sup>	2.263(3)
Zn(1)-N(4) <sup>2</sup>	2.027(3)	Zn(1)-N(4)	2.027(3)
Zn(1)-N(5) <sup>2</sup>	2.170(3)	Zn(1)-N(5)	2.170(3)
O(2)-Zn(1)-O(2) <sup>2</sup>	180.00(19)	N(4) <sup>2</sup> -Zn(1)-O(2) <sup>2</sup>	94.81(11)
N(4)-Zn(1)-O(2) <sup>2</sup>	85.19(11)	N(4) <sup>2</sup> -Zn(1)-O(2)	85.19(11)
N(4)-Zn(1)-O(2)	94.81(11)	N(4)-Zn(1)-N(4) <sup>2</sup>	180.0
N(4) <sup>2</sup> -Zn(1)-N(5) <sup>2</sup>	77.67(12)	N(4) <sup>2</sup> -Zn(1)-N(5) <sup>2</sup>	102.33(12)
N(4)-Zn(1)-N(5) <sup>2</sup>	102.33(12)	N(4)-Zn(1)-N(5)	77.67(12)
N(5)-Zn(1)-O(2)	83.49(11)	N(5) <sup>2</sup> -Zn(1)-O(2) <sup>2</sup>	83.49(11)
N(5) <sup>2</sup> -Zn(1)-O(2)	96.51(11)	N(5)-Zn(1)-O(2) <sup>2</sup>	96.51(11)
N(5)-Zn(1)-N(5) <sup>2</sup>	180.00(9)	N(3)-N(4)-Zn(1)	133.8(2)
C(9)-N(4)-Zn(2)	116.1(2)	C(10)-N(5)-Zn(1)	114.0(2)

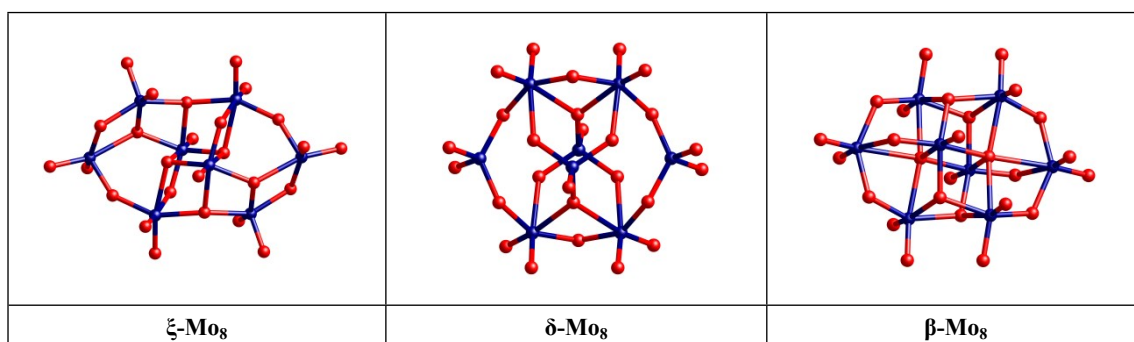
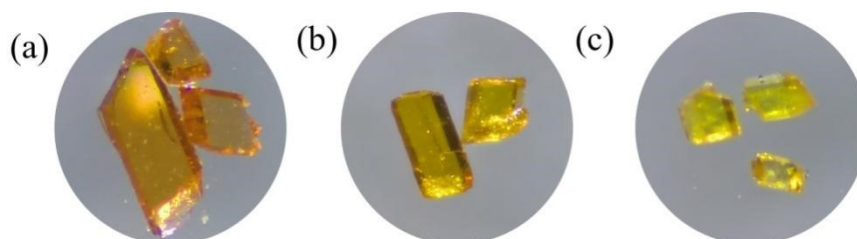
Symmetry codes: <sup>1</sup>1-X,1-Y,1-Z; <sup>2</sup>1-X,2-Y,1-Z

**Table S3.** The sizes and charge of the selected dyes.

Name	Anionic	Cationic			
	MO	RhB	NR	MB	CV
Structural formula					
charge	-1	+1	+1	+1	+1
x(Å)	4.5	6.8	3.8	1.8	3.5
y(Å)	6.0	11.8	6.9	5.5	13.0
z(Å)	14.8	15.8	14.8	14.2	13.7

**Table S4.** Comparison of the photocatalytic reduction of Cr(VI) by different photocatalysts.

Catalyst	$C_{\text{catalyst}}$ ( $\text{g}\cdot\text{L}^{-1}$ ) 1)	Time (min)	Degradation Rate (%)	Ref.
Compounds <b>1</b>	0.40	30	95.85%	This work
Compounds <b>2</b>	0.40	30	93.99%	This work
Compounds <b>3</b>	0.40	30	90.29%	This work
Compounds <b>4</b>	0.40	30	88.18%	This work
UiO-66-NH <sub>2</sub>	0.40	30	51.6%	30
[Cu <sub>2</sub> (Cmt) <sub>2</sub> (OH)Cl][( $\beta$ -Mo <sub>8</sub> O <sub>26</sub> ) <sub>0.5</sub> ]	0.20	60	54.3%	53
C <sub>3</sub> N <sub>4</sub> (5.0 wt.%)/ZnO	—	100	75.5%	54
Zr-MOF	0.25	60	73%	55
50AH-CN	0.50	150	56%	56

**Fig. S1.** Three isomers of octamolybdate contained in compounds 1–4.**Fig. S2.** Contrast photos of crystal colors of compounds **1** (a), **2** (b) and **3** (c).

Compound <b>1</b>	Compound <b>2</b>	Compound <b>3–4</b>
-------------------	-------------------	---------------------

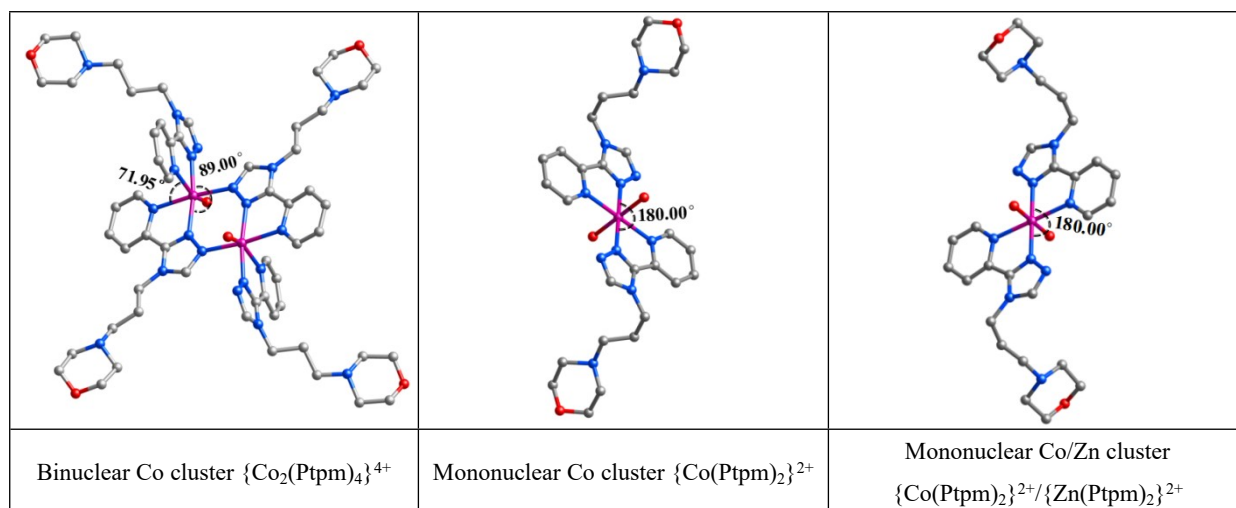


**Fig. S3.** Binuclear and mononuclear metal clusters formed by connecting metal atoms with ptpm ligand in compounds 1–4.

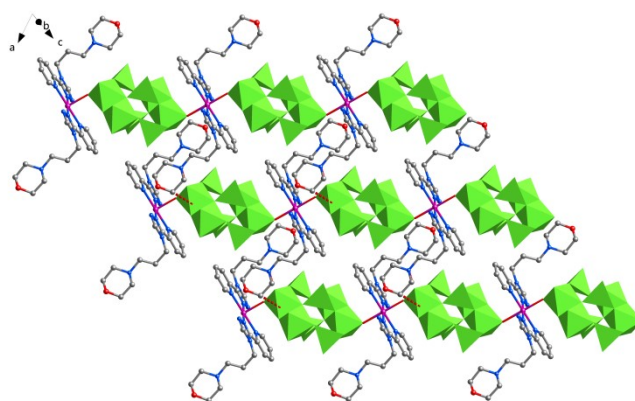


**Fig. S4.** The 2D supramolecular layer of compound 2.

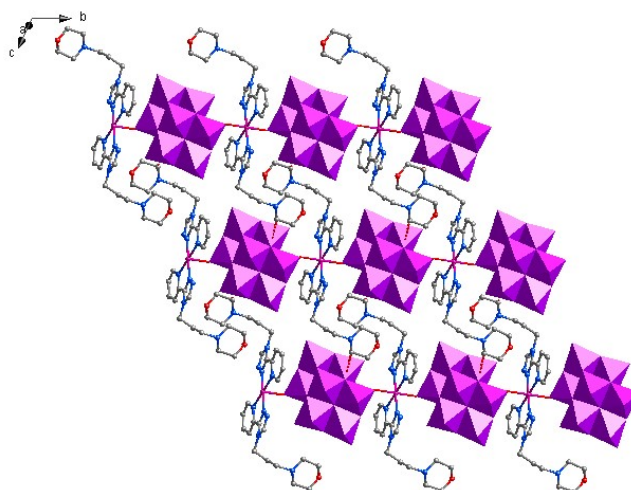


**Fig. S5.** The 2D supramolecular layer of compound 3.

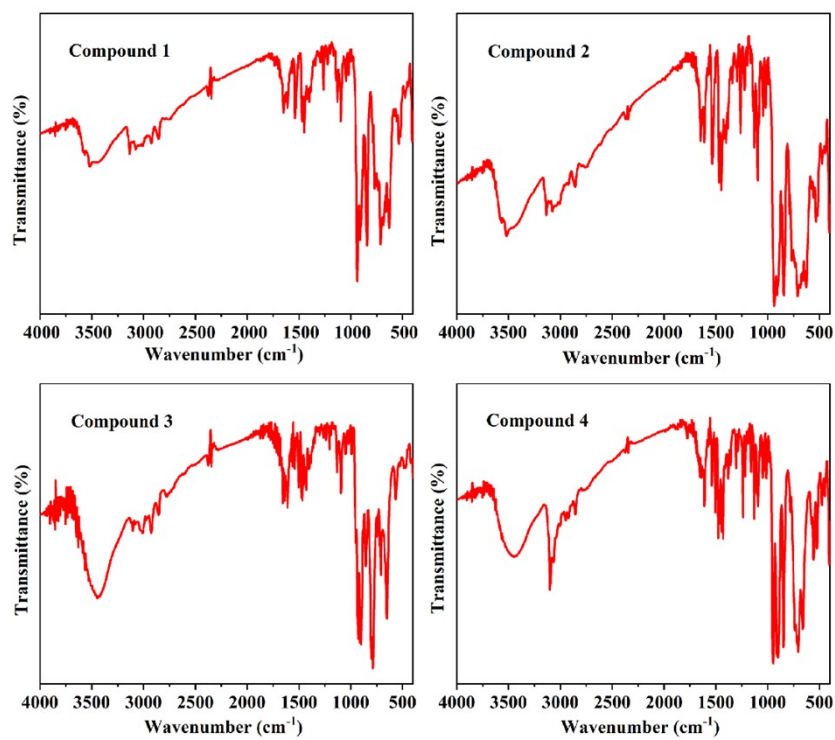


Fig. S6. The IR spectra of compounds 1–4.

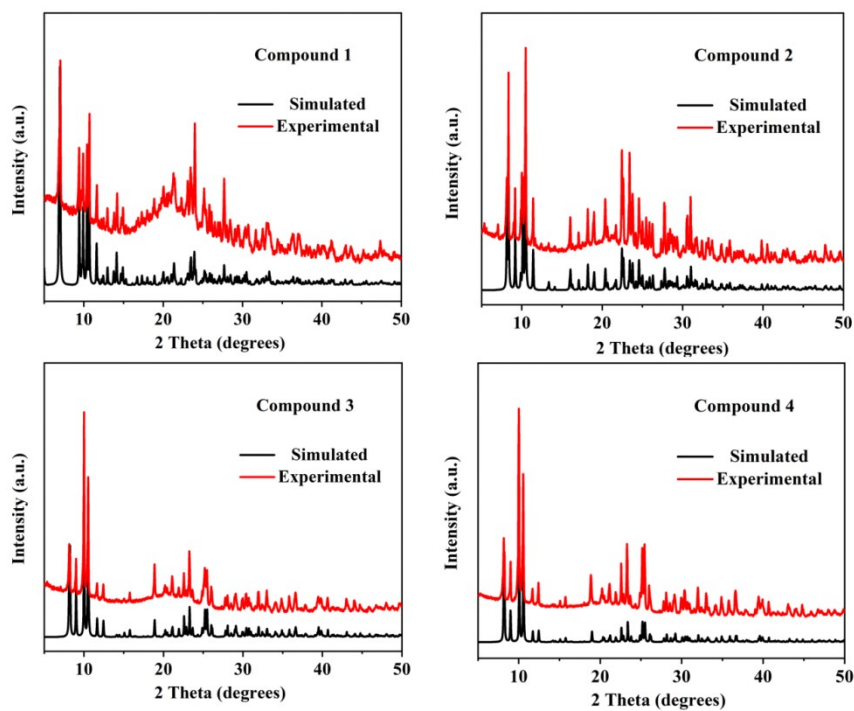
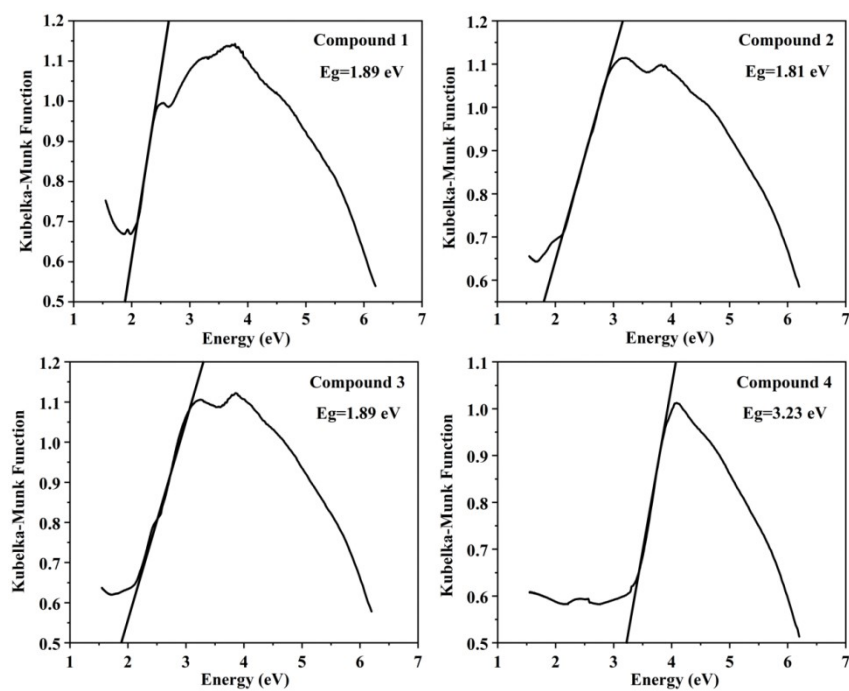
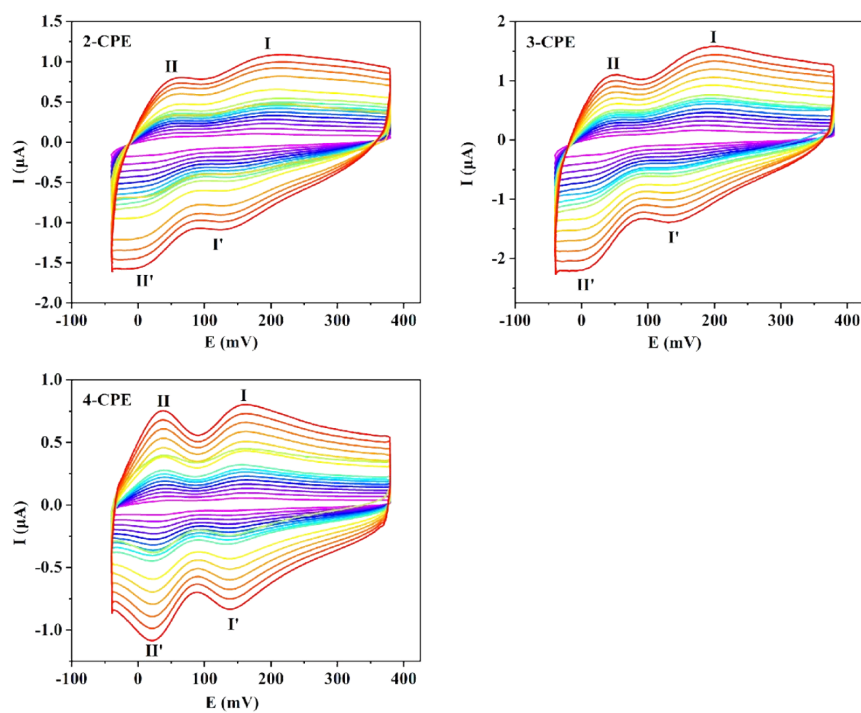


Fig. S7. The PXRD of compounds 1–4.





**Fig. S8.** Solid-state optical diffuse-reflection spectra of compounds 1–4.



**Fig. S9.** The CV of 2– to 4-CPEs in the electrolyte solution ( $20\text{--}500\text{ mV s}^{-1}$ ).

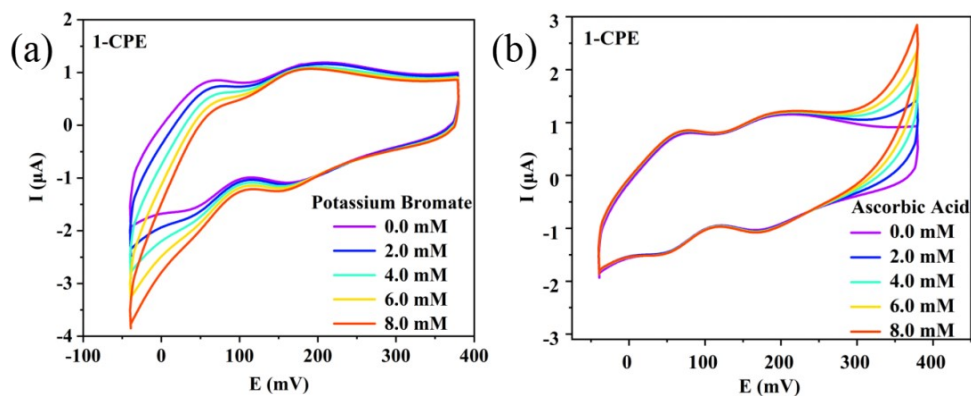


**Fig. S10.** Cyclic voltammogram of **1**-CPE in 0.1 M H<sub>2</sub>SO<sub>4</sub> + 0.5 M Na<sub>2</sub>SO<sub>4</sub> solution containing 0–8 mM KBrO<sub>3</sub>/AA at a scanning rate of 200 mV s<sup>-1</sup>.

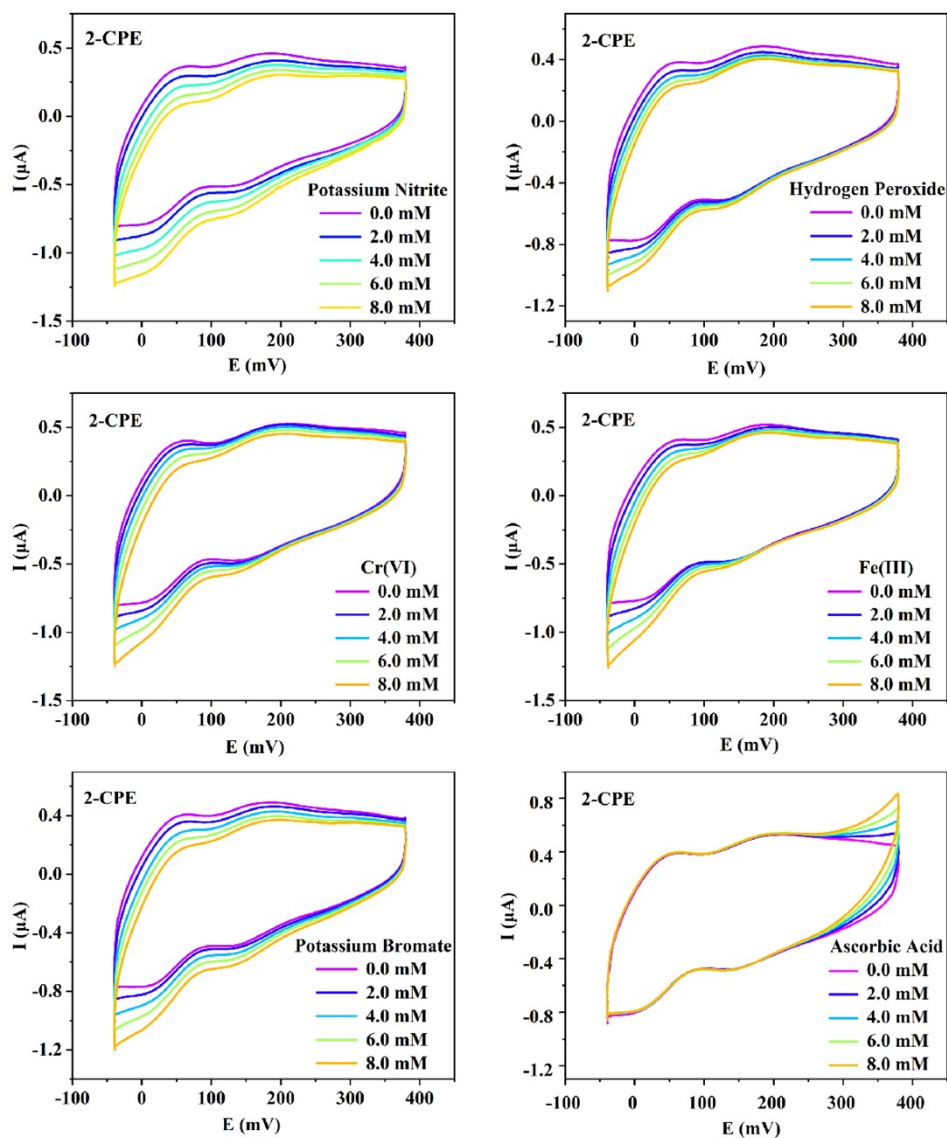


**Fig. S11.** Cyclic voltammogram of **2**-CPE in 0.1 M H<sub>2</sub>SO<sub>4</sub> + 0.5 M Na<sub>2</sub>SO<sub>4</sub> solution containing 0–8 mM KNO<sub>2</sub>/H<sub>2</sub>O<sub>2</sub>/Cr(VI)/Fe(III)/KBrO<sub>3</sub>/AA at a scanning rate of 200 mV s<sup>-1</sup>.

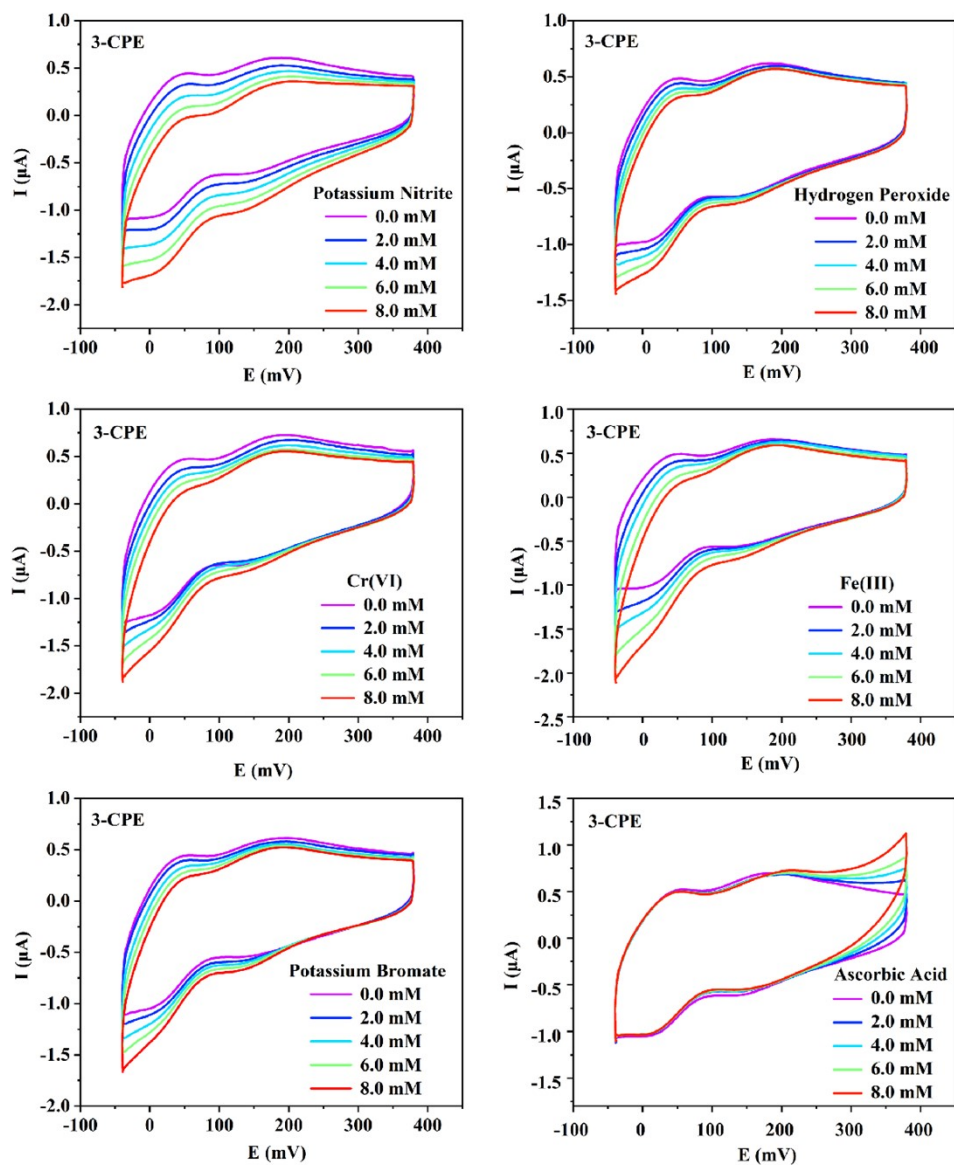


**Fig. S12.** Cyclic voltammogram of 3-CPE in 0.1 M  $\text{H}_2\text{SO}_4$  + 0.5 M  $\text{Na}_2\text{SO}_4$  solution containing 0–8 mM  $\text{KNO}_2/\text{H}_2\text{O}_2/\text{Cr(VI)}/\text{Fe(III)}/\text{KBrO}_3/\text{AA}$  at a scanning rate of  $200 \text{ mV s}^{-1}$ .

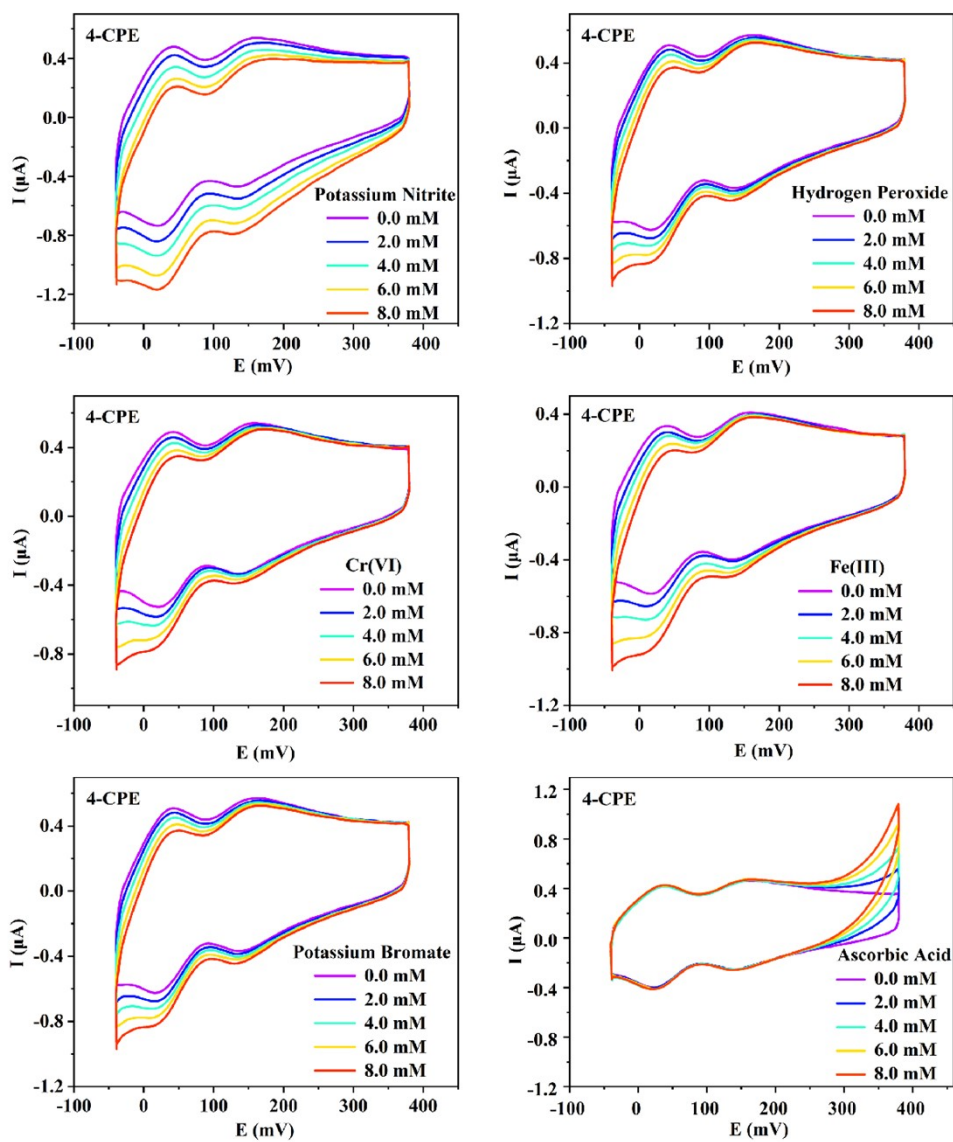


**Fig. S13.** Cyclic voltammogram of 4-CPE in 0.1 M H<sub>2</sub>SO<sub>4</sub> + 0.5 M Na<sub>2</sub>SO<sub>4</sub> solution containing 0–8 mM KNO<sub>2</sub>/H<sub>2</sub>O<sub>2</sub>/Cr(VI)/Fe(III)/KBrO<sub>3</sub>/AA at a scanning rate of 200 mV s<sup>-1</sup>.

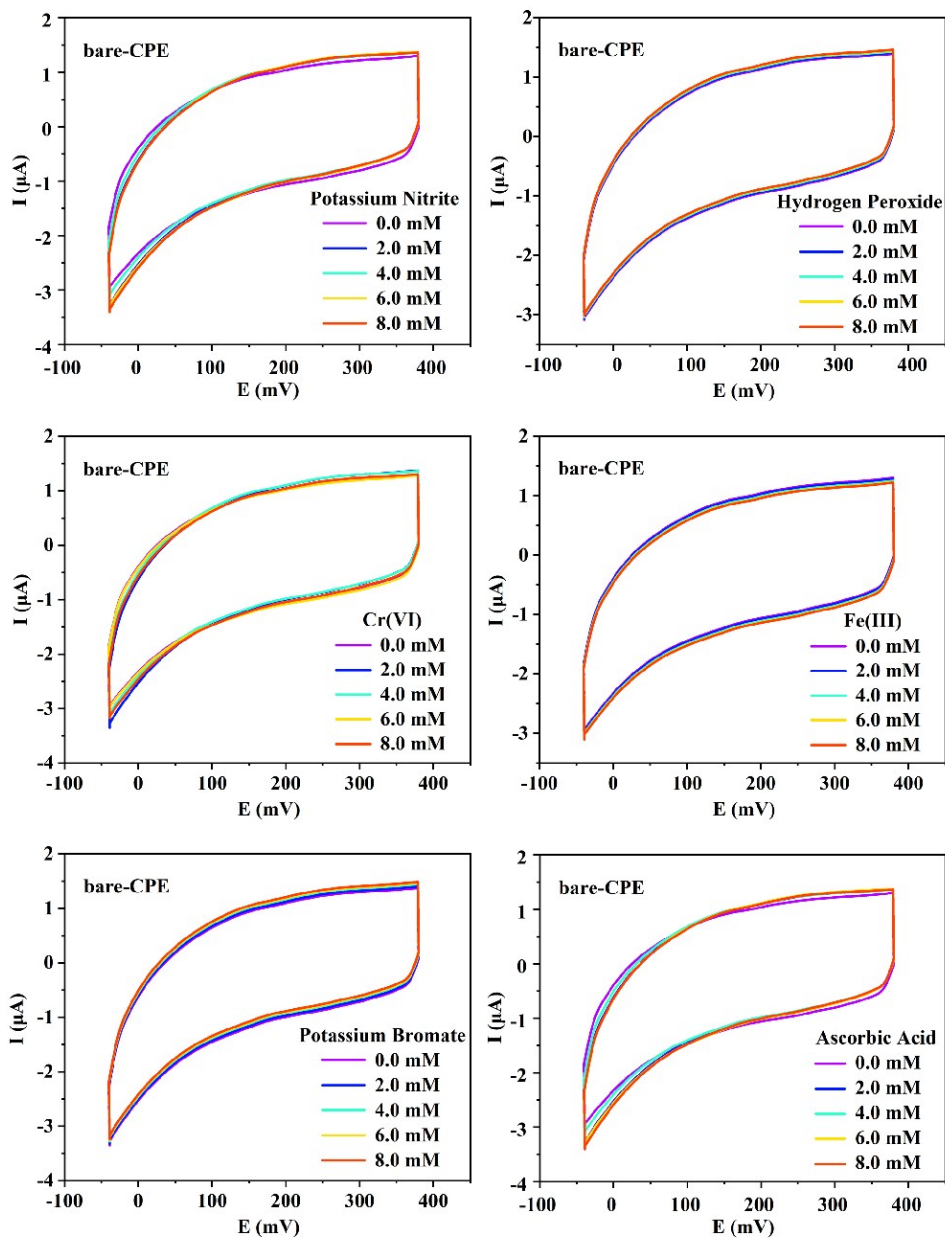


**Fig. S14.** Cyclic voltammogram of bare-CPE in 0.1 M  $\text{H}_2\text{SO}_4$  + 0.5 M  $\text{Na}_2\text{SO}_4$  solution containing 0–8 mM  $\text{KNO}_2/\text{H}_2\text{O}_2/\text{Cr(VI)}/\text{Fe(III)}/\text{KBrO}_3/\text{AA}$  at a scanning rate of  $200 \text{ mV s}^{-1}$ .

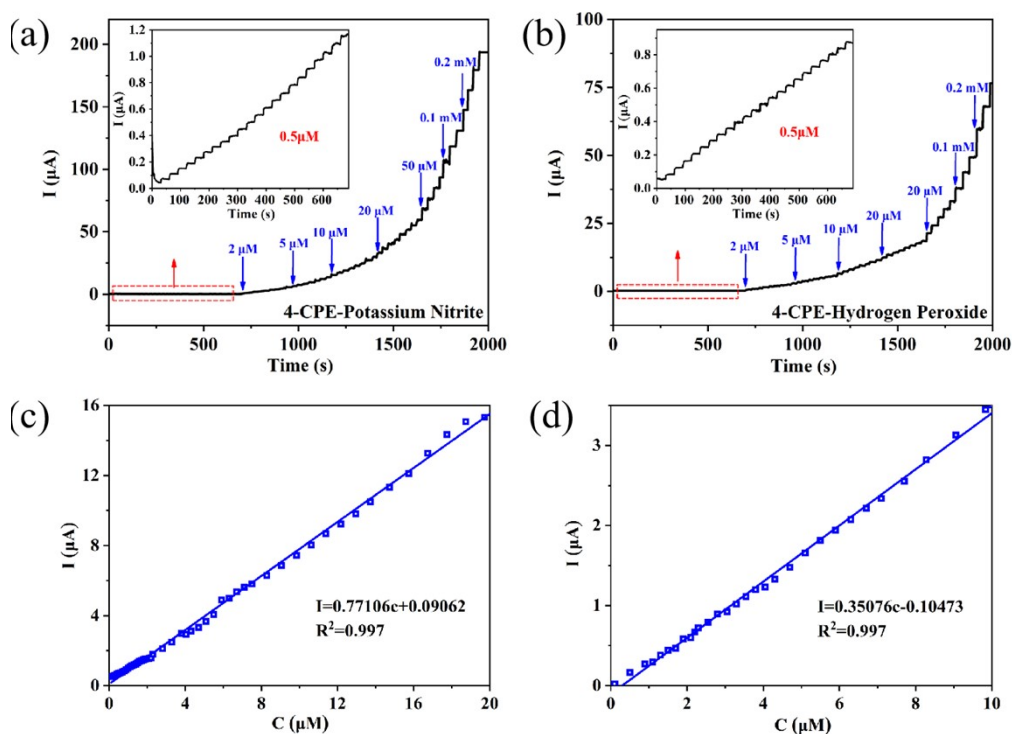


**Fig. S15.** I-T curve of adding  $\text{KNO}_2$  (a) and  $\text{H}_2\text{O}_2$  (b) continuously in the electrolyte solution; Calibration diagram of current and concentration of  $\text{KNO}_2$  (c) and  $\text{H}_2\text{O}_2$  (d) detected by 4-CPE.

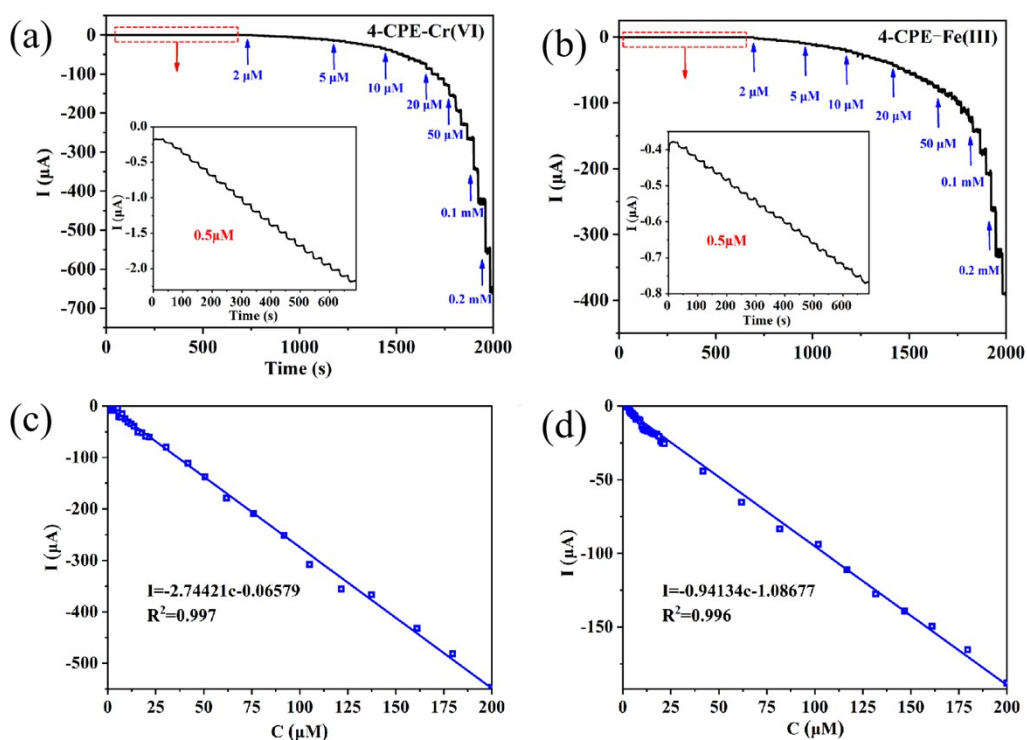


**Fig. S16.** I-T curve of adding  $\text{Cr(VI)}$  (a) and  $\text{Fe(III)}$  (b) continuously in the electrolyte solution; Calibration diagram of current and concentration of  $\text{Cr(VI)}$  (c) and  $\text{Fe(III)}$  (d) detected by 4-CPE.

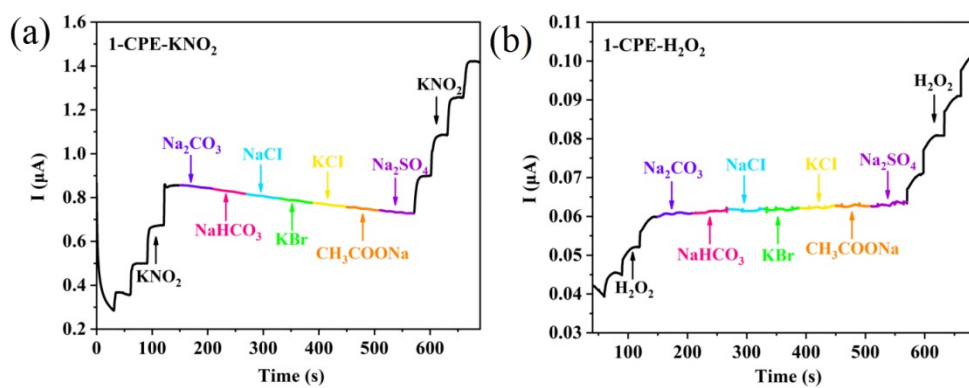


**Fig. S17.** Interference of the successive addition of different metal ions ( $\text{CO}_3^{2-}$ ,  $\text{Cl}^-$ ,  $\text{HCO}_3^-$ ,  $\text{Br}^-$ ,  $\text{CH}_3\text{COO}^-$  and  $\text{SO}_4^{2-}$ ) in 0.1 M  $\text{H}_2\text{SO}_4$  + 0.5 M  $\text{Na}_2\text{SO}_4$  aqueous solution.

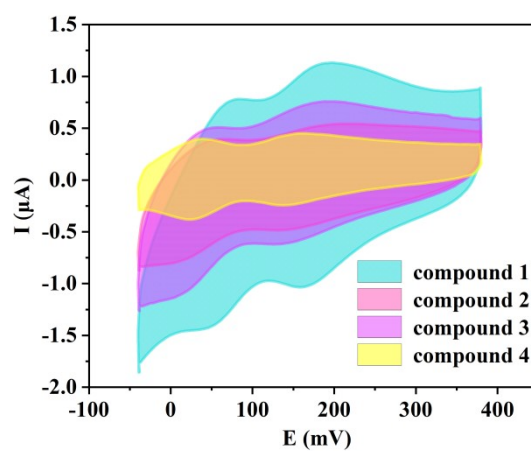


**Fig. S18.** Comparative diagrams of CV curve at 200 mV s<sup>-1</sup>.

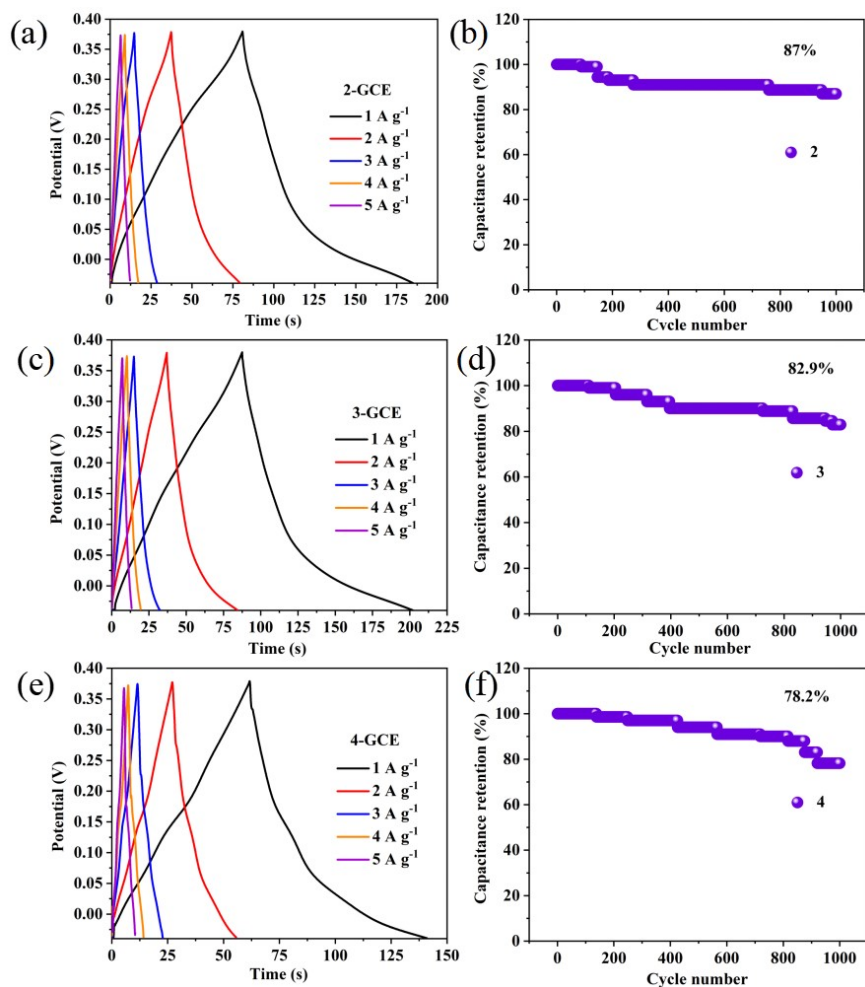


**Fig. S19.** (a), (c) and (e) GCD curves of the 2-, 3- and 4-GCE, respectively (current densities: of 1, 2, 3, 4, and 5  $A \cdot g^{-1}$ ). (b), (d) and (f) Corresponding to their cyclic stability in 2000 cycles, respectively (current density: 5  $A \cdot g^{-1}$ ).

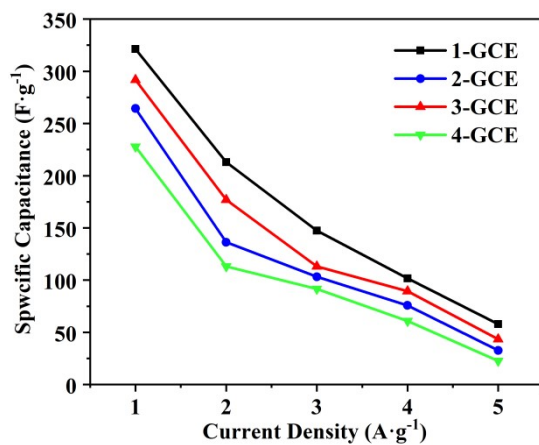


**Fig. S20.** The variation of capacitance for 1-, 2-, 3- and 4-GCE with current density.



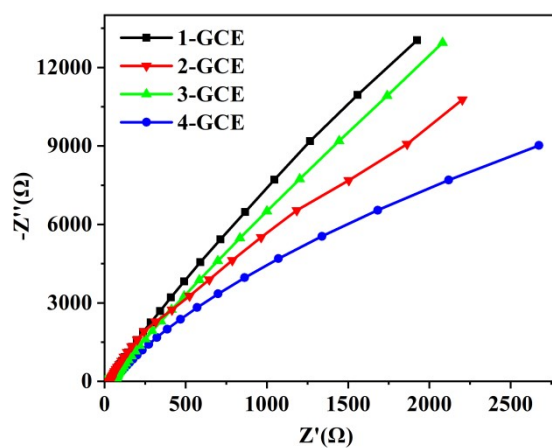


**Fig. S21.** EIS contrast spectra of 1–, 2–, 3– and 4–GCE in a 0.1 M  $\text{H}_2\text{SO}_4$  solution (at low frequency region).

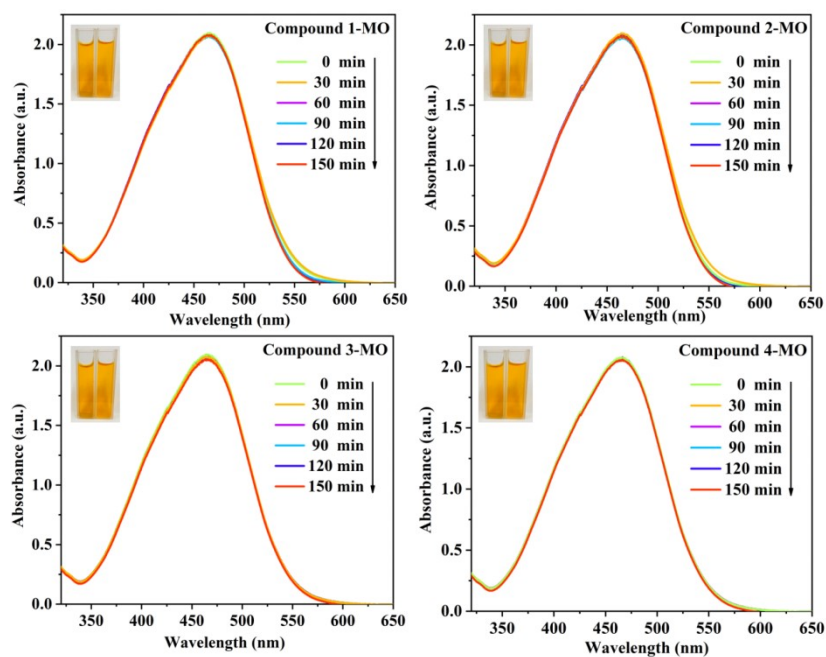


**Fig. S22.** UV-vis spectra of the MO with compounds 1–4 as adsorbents (illustration: color change of dye solution before and after crystal adsorption).

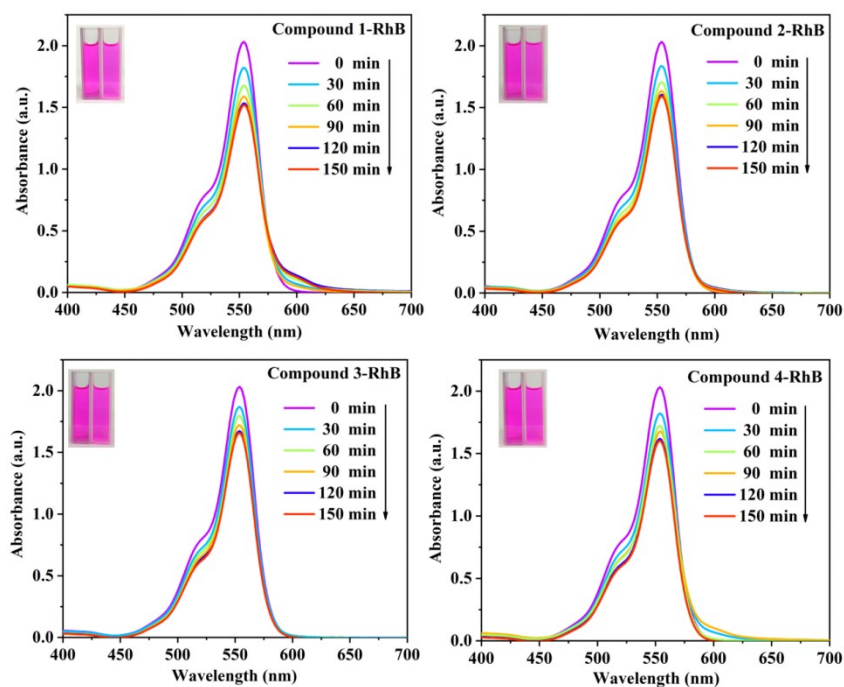


**Fig. S23.** UV-vis spectra of the RhB with compounds 1–4 as adsorbents (illustration: color change of dye solution before and after crystal adsorption).

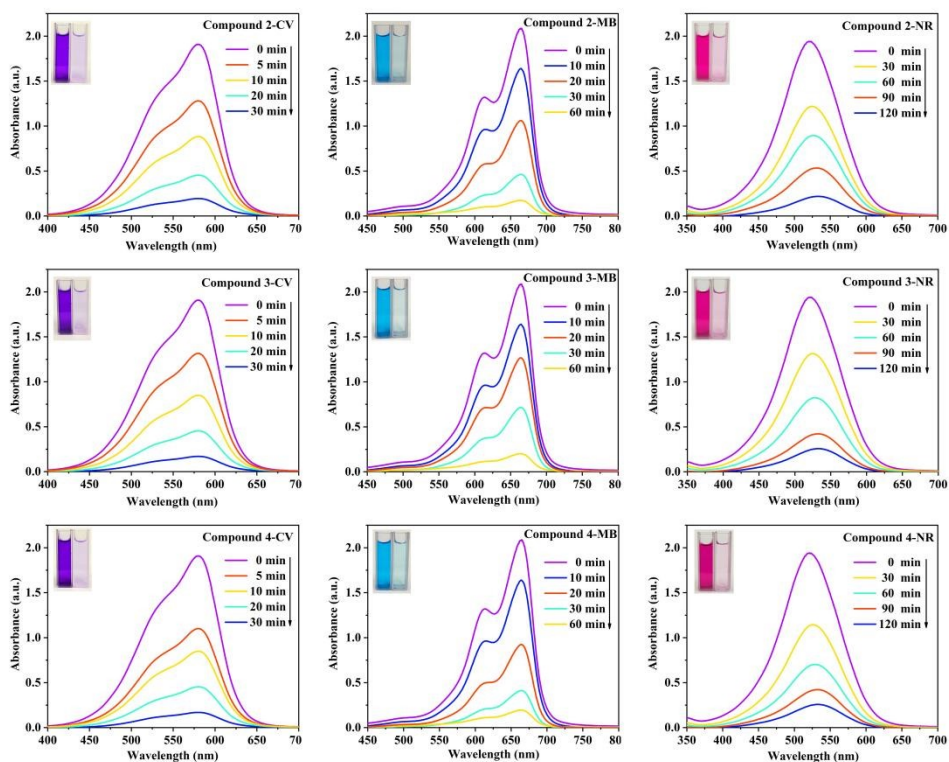


**Fig. S24.** UV-vis spectra of the CV, MB, and NR with compounds 2–4 as adsorbents (illustration: color change of dye solution before and after crystal adsorption).

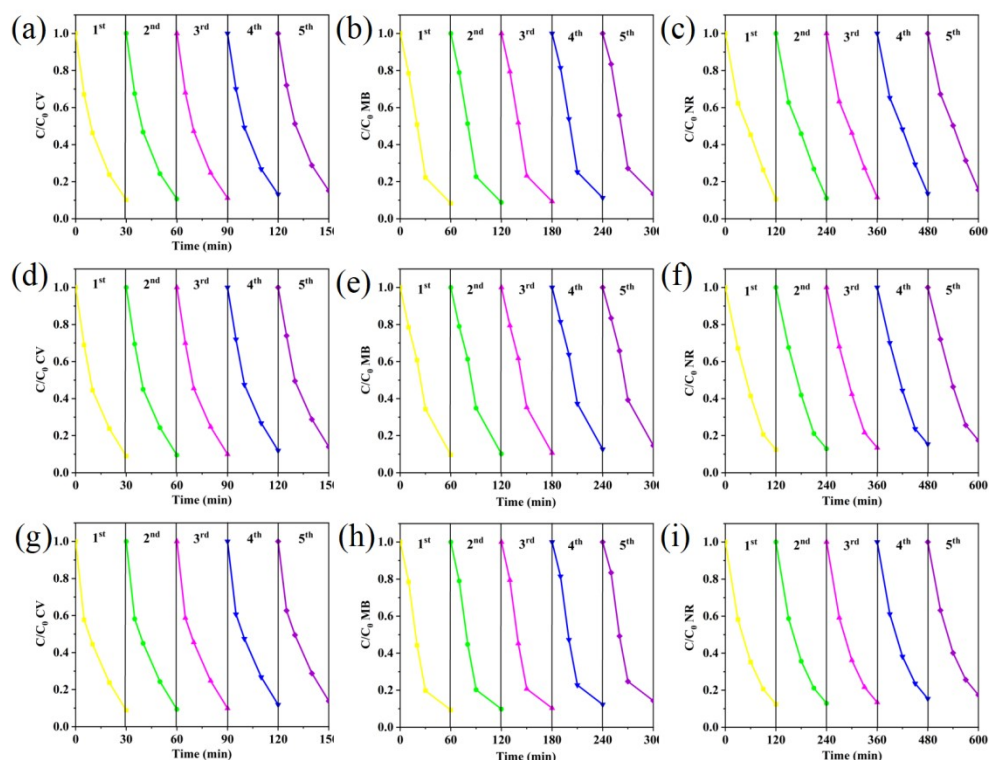


**Fig. S25.** Five adsorption-desorption cycle tests of compound **2** (a)–(c), **3** (d)–(f), **4** (g)–(i) for CV, MB and NR.

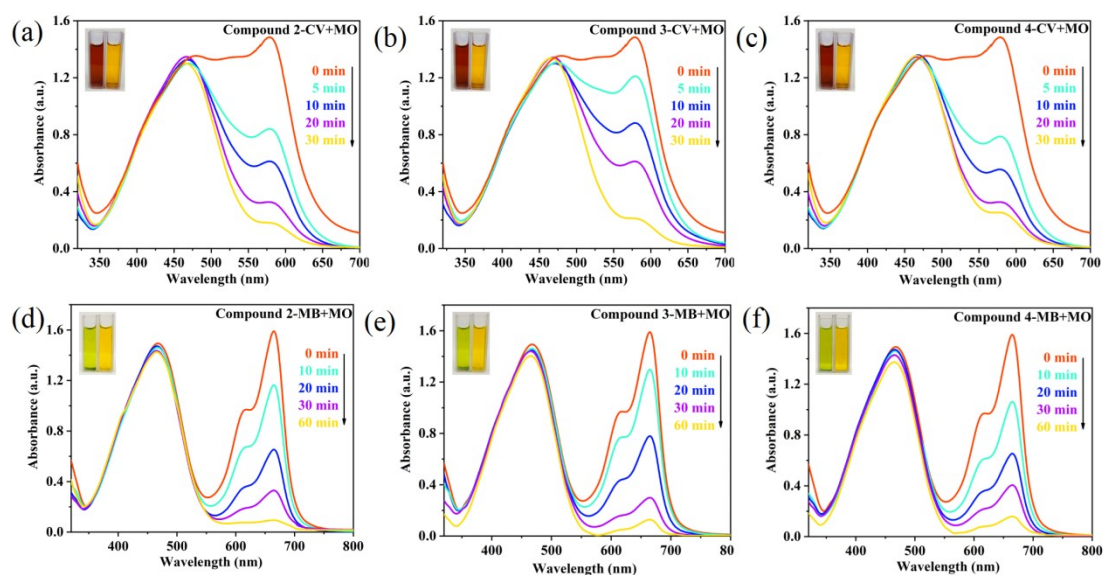


**Fig. S26.** UV-vis spectra of compounds **2–4** in the adsorption of mixed dye solutions: (a)–(c) CV/MO, (d)–(f)

MB/MO.

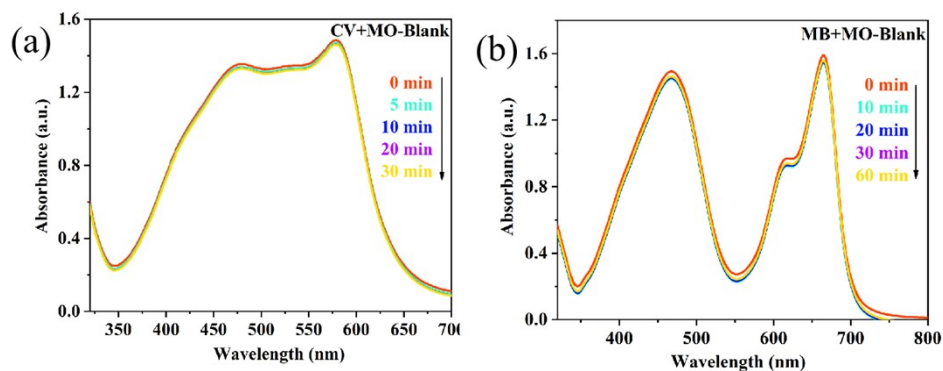


Fig. S27. UV/vis spectra of the binary mixed dyes without adsorbents: CV/MO (a) and MB/MO (b).

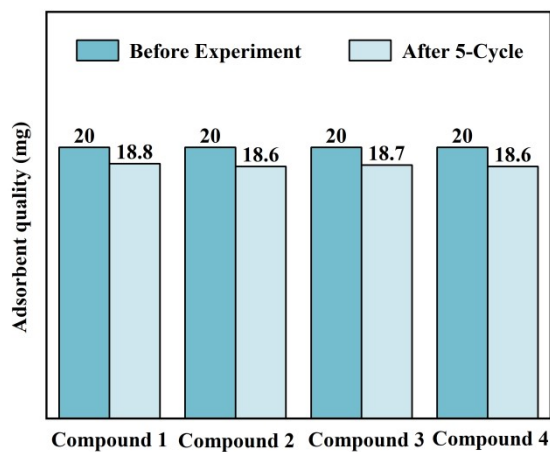


Fig. S28. Quality of adsorbent before and after five cycles.

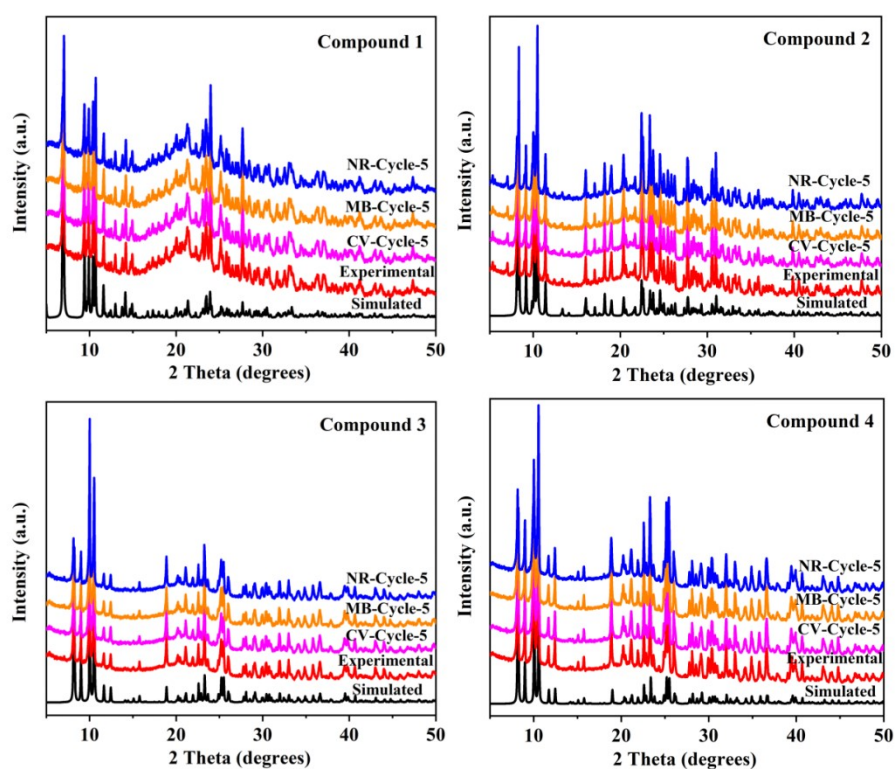


Fig. S29. PXRD pattern of complexes 1–4 after five cycles of adsorption test.

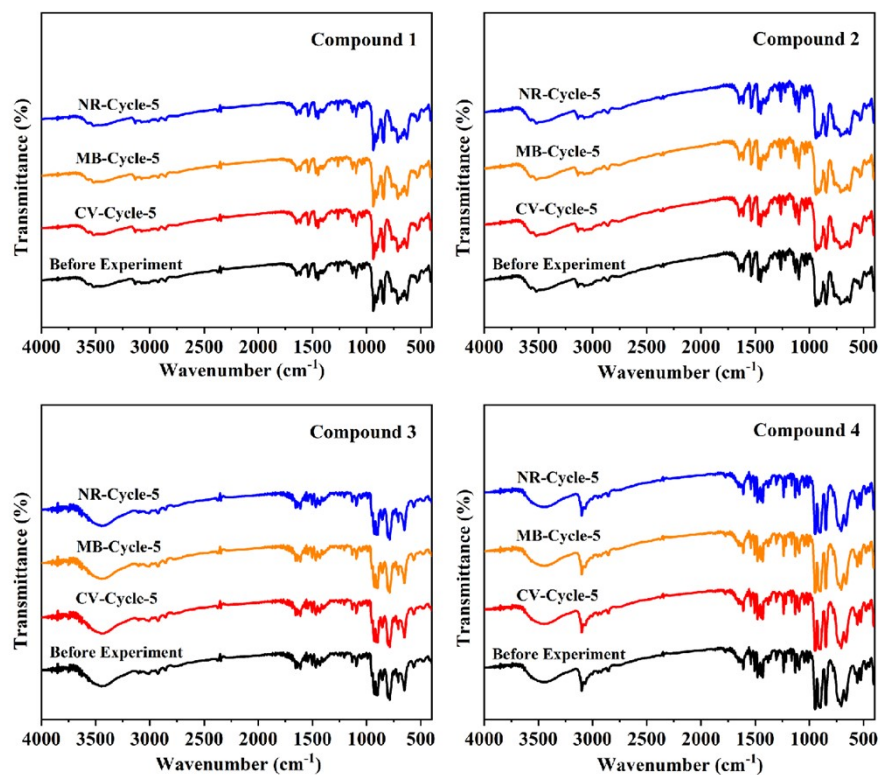


Fig. S30. The IR spectra of compounds 1–4 after five cycles of adsorption test.

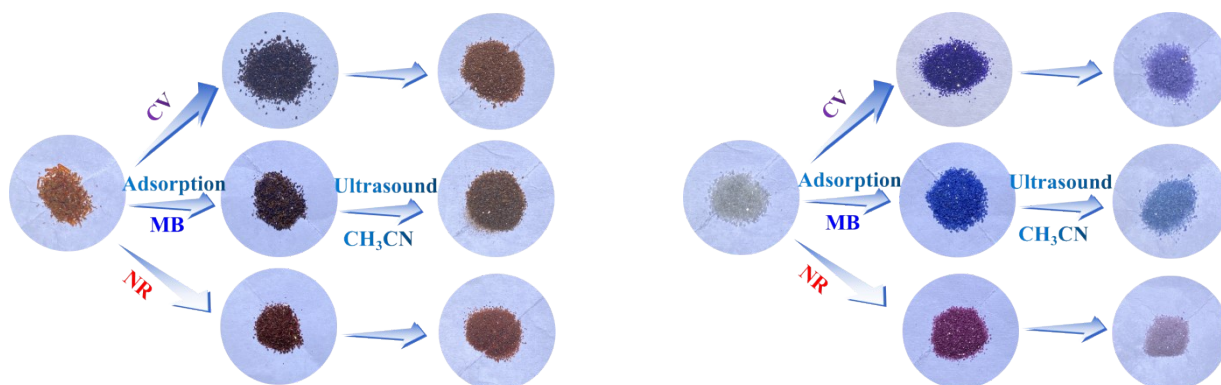


Fig. S31. Color photos of adsorption-desorption of compound 1 (left) and compound 4 (right).

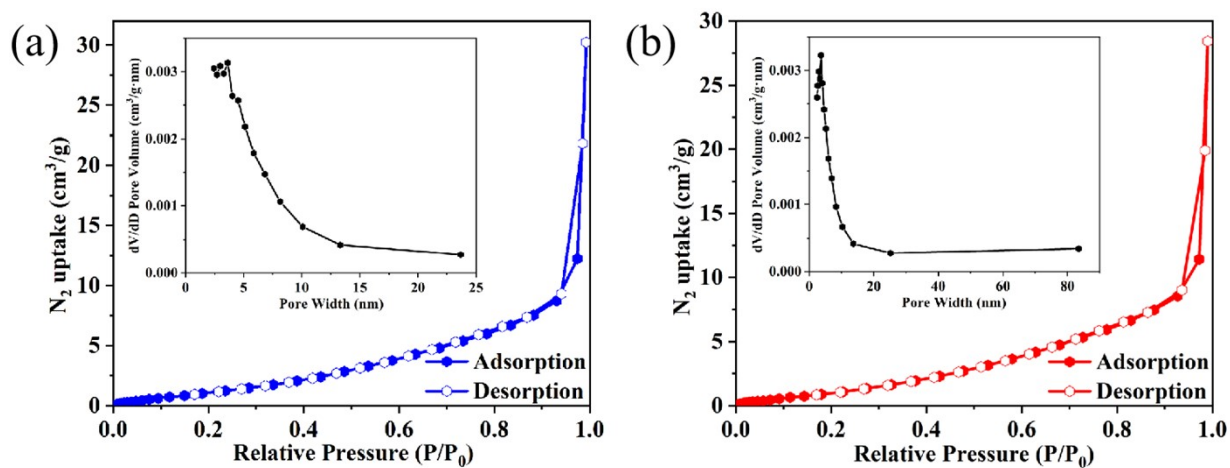


Fig. S32. N<sub>2</sub> adsorption isotherm of compound 1 (a) and compound 4 (b) (inset: BJH Desorption dV/dD Pore Volume

plot of corresponding compounds 1 and 4).

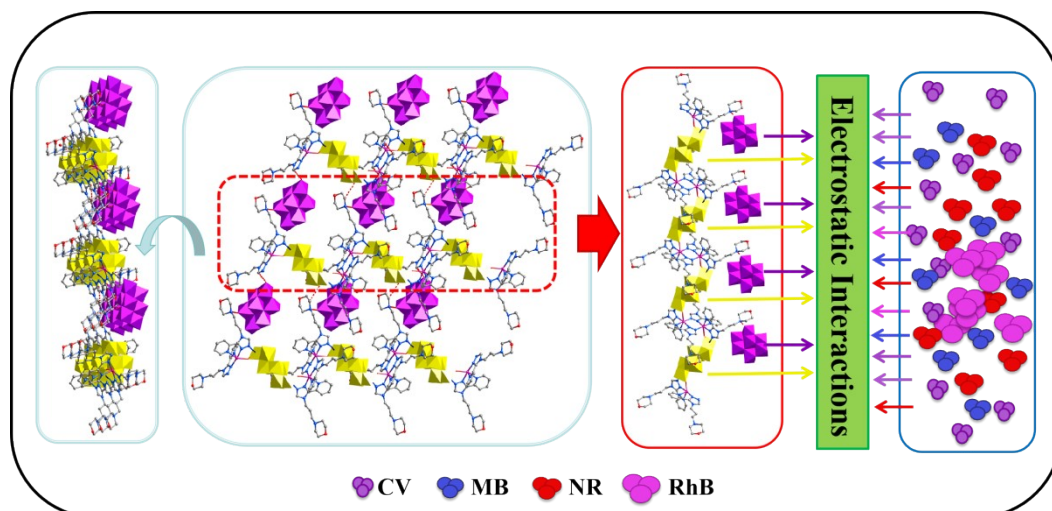


Fig. S33. Schematic representation of possible dye adsorption mechanism in 1.

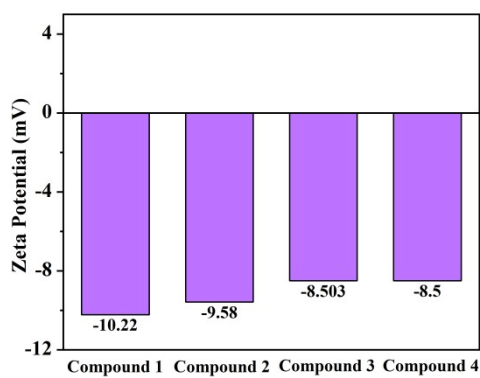


Fig. S34. The zeta potential of compounds 1–4.

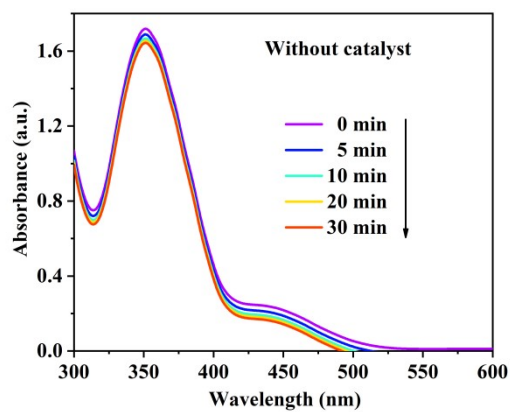
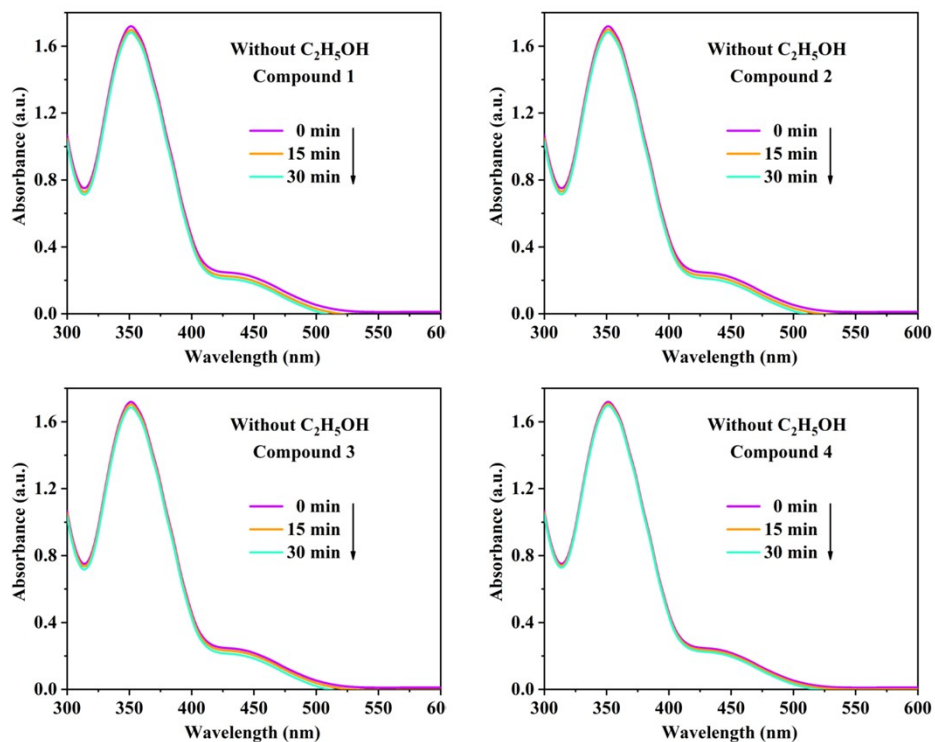
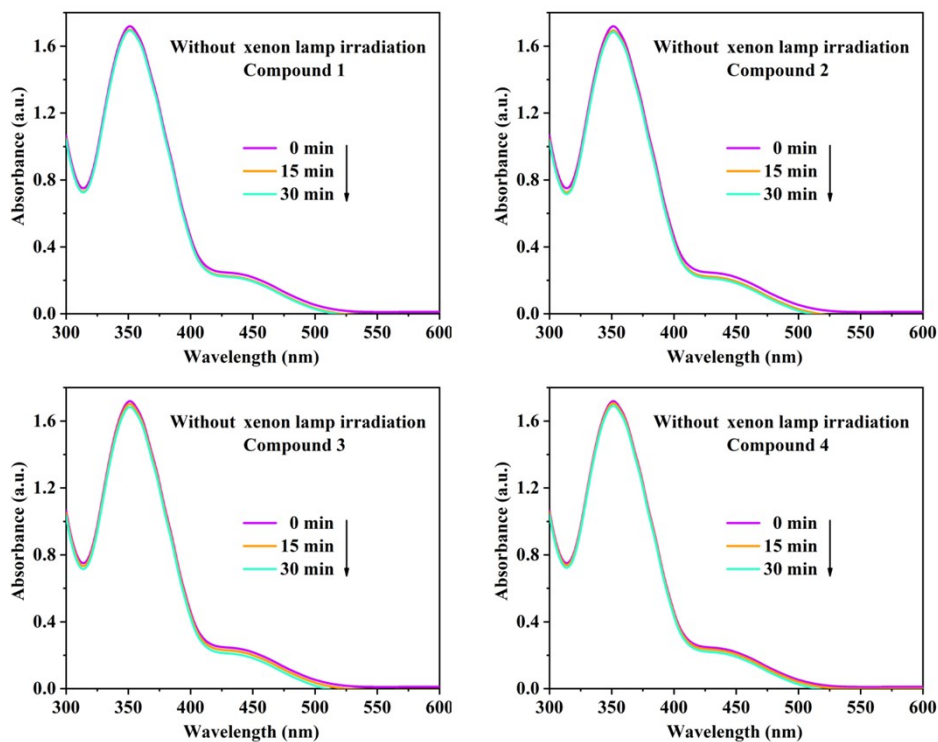


Fig. S35. The UV spectra of the Cr(VI) solution without adding catalyst.



**Fig. S36.** The UV spectra of Cr(VI) solution without C<sub>2</sub>H<sub>5</sub>OH.



**Fig. S37.** The UV spectra of Cr(VI) solution without 300W xenon lamp irradiation.

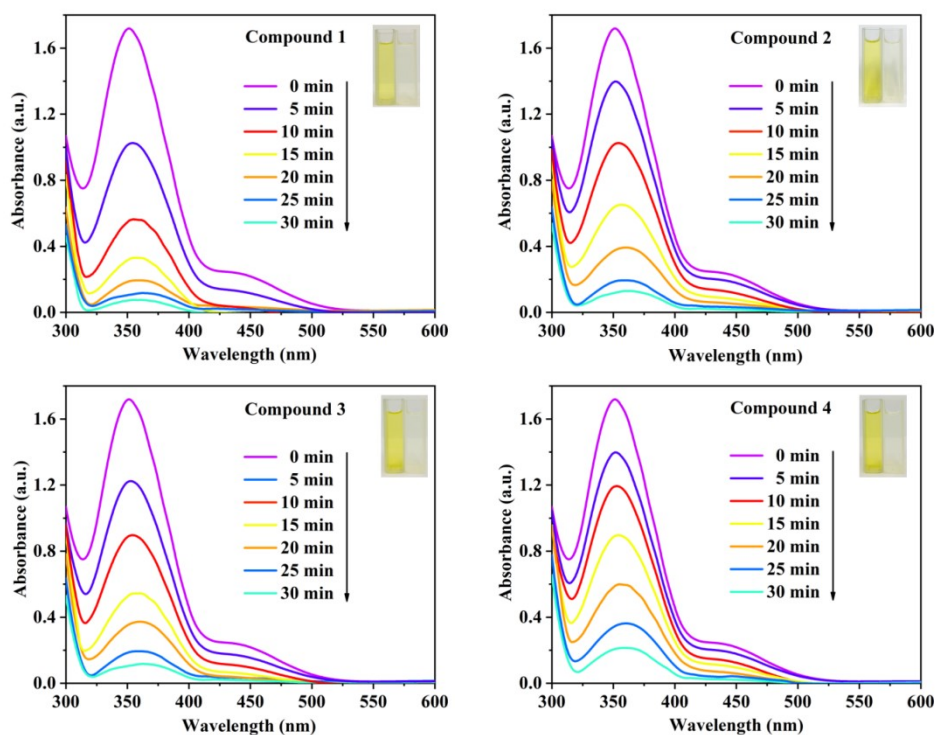


**Fig. S38** Under 300W xenon lamp irradiation ( $300 \leq \lambda \leq 400$  nm), ultraviolet spectrum of Cr(VI) solution with compounds 1–4 as photoreduction catalyst .

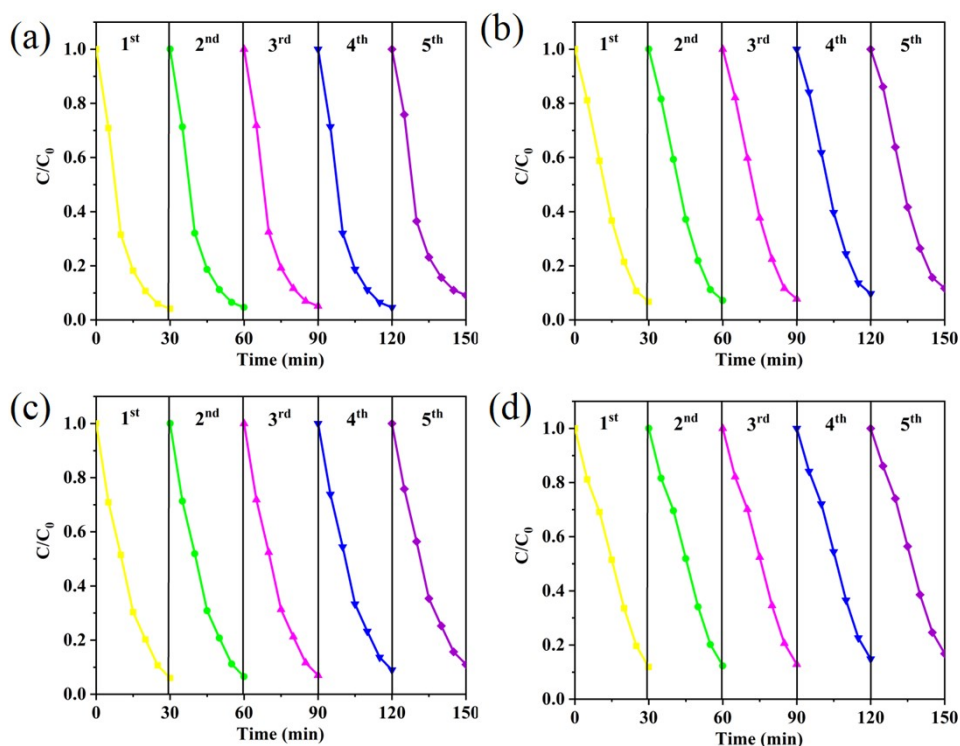


**Fig. S39** Five cycles of photocatalytic reduction of compounds 1–4.



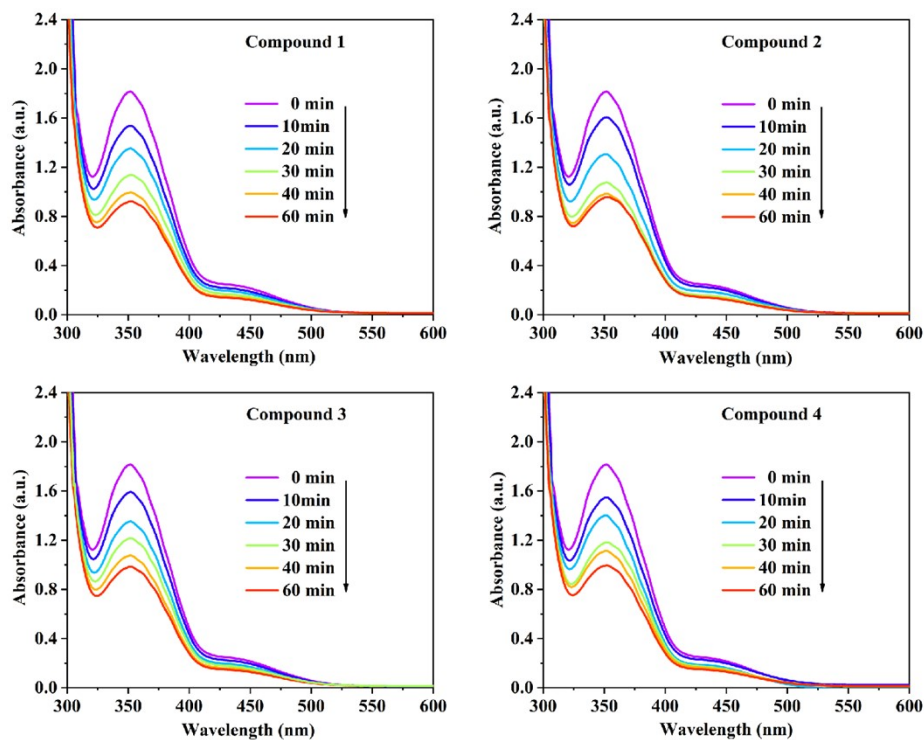


**Fig. S40** Under 300 W xenon lamp irradiation (300  $\square$   $\lambda$   $\square$  400 nm), ultraviolet spectra of Cr(VI) solution with compounds 1-4 as photoreduction catalyst.

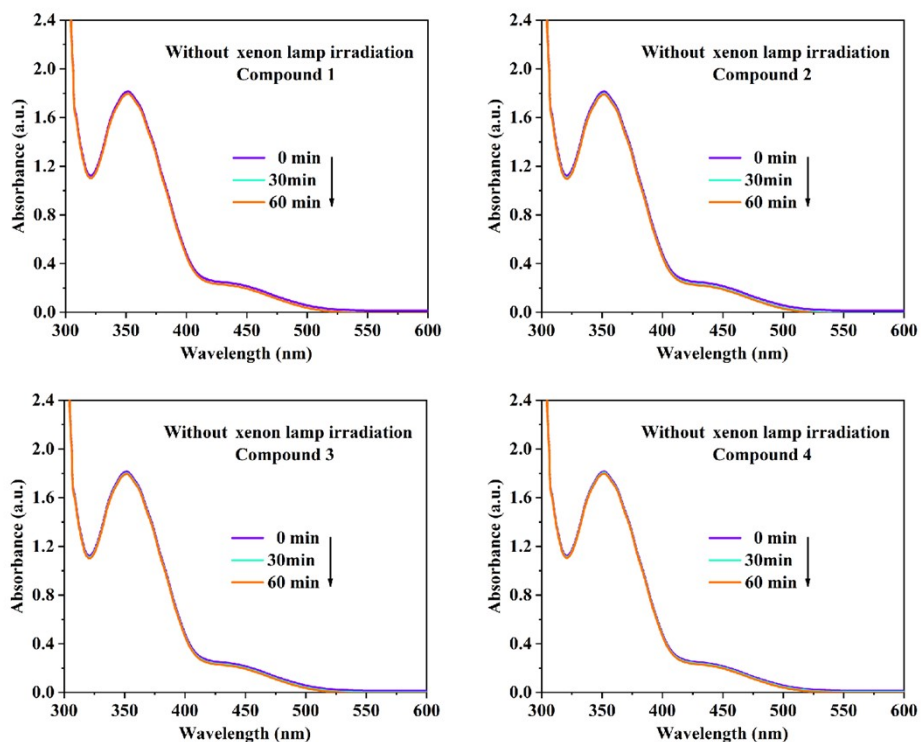


**Fig. S41** The UV spectra of Cr(VI) solution without 300W xenon lamp irradiation.

## References

- 1 O. V. Dolomanov, L. J. Bourhis, R. J. Gildea, J. A. K. Howard and H. Puschmann, *J. Appl. Crystallogr.*, 2009, **42**, 339.